Available online at www.sciencedirect.com
SCIENCE DIRECT®
Journal of Magnetism and Magnetic Materials 302 (2006) 334–339
Journal of magnetism and magnetic materials
www.elsevier.com/locate/jmmm

Granule size and shape influence on static and dynamic properties of magnetic nanocomposites

T.V. Bagmut[a], S.V. Nedukh[a], S.T. Roschenko[b], I.G. Shipkova[b], S.I. Tarapov[a,*]

[a]*Institute of Radiophysics and Electronics NAS of Ukraine, 12 Ac. Proskura St., Kharkov 61085, Ukraine*
[b]*Kharkov Polytechnical Institute, National Technical University, 21 Frunze St., Kharkov 61002, Ukraine*

Received 16 May 2005; received in revised form 11 September 2005
Available online 7 October 2005

Abstract

Static and dynamic magnetic properties are examined for granular systems $Co_x(TiO_2)_{1-x}$ with Co volumetric contents of 31.6, 41.4, 49.4 and 57.6 vol%. The ferromagnetic resonance (FMR) technique in the 38–45 GHz band and the vibrating sample magnetometer technique were applied. The results from comparative analysis of saturation magnetization defined by both methods are discussed and the estimation of the most probable sizes and shapes of magnetic particles forming the nanocomposite is carried out.
© 2005 Elsevier B.V. All rights reserved.

PACS: 73.40.Gk; 72.15.Gd; 78.20.Ls

Keywords: Granular magnetic nanocomposites; Ferromagnetic resonance; Superparamagnetism; Langevin function

1. Introduction

Granular nanomaterials with a tunneling magnetoresistance (TMR) effect [1,2] composed of magnetic metals embedded into insulator matrix are being investigated intensively because of their future prospects for microwave applications. An objective of these investigations is the definition of the conditions which allow combining together in one specimen both a high value of TMR ratio and a relatively small magnetizing field. The large TMR ratio was found in systems consisting of Co granules embedded in dielectric matrix of Al_2O_3, MgF_2, SiO_2 and TiO_2 [1–4]. Though the important correlation was observed between Co volumetric contents and both the maximal TMR ratio and TMR magnetic field dependence, parameter such as the granule volumetric content does not permit to interpret the obtained results correctly. It follows from the fact that real granular systems are very complicated objects with granules of various sizes and shapes.

Taking into a consideration the ferromagnetism of Co granules, various magnetic interactions can play an important role in such systems [5]. To explain the experimental results, it is necessary to construct a model that represents the system most adequately. In this paper, we discuss the possibilities of magnetic static and dynamic measuring methods for investigation of characteristics of granular systems which will form the basis of adequate models.

2. Experimental methods

The granular systems $Co_x(TiO_2)_{1-x}$ with Co volumetric contents of 31.6, 41.4, 49.4 and 57.6 vol% have been studied. These specimens exhibit the TMR phenomenon of noticeable magnitude (Table 1). The samples have been made in the Laboratory for Advanced Spin Electronics Researches (Toyohashi University of Technology) using RF magnetron sputtering in the Ar atmosphere. The tandem deposition method was employed. Using this method, the Co and TiO_2 layers were deposited in series one after another during substrate rotation over Co and TiO_2 targets. The speed of rotation was sufficiently high to prevent continuous film formation. As a result, the system

*Corresponding author. Tel./fax: 38 057 7 441 105.
E-mail address: tarapov@ire.kharkov.ua (S.I. Tarapov).

0304-8853/$ - see front matter © 2005 Elsevier B.V. All rights reserved.
doi:10.1016/j.jmmm.2005.09.028

Table 1

Specimen #	1	2	3	4
Co, X vol%	31.6	41.4	49.4	57.6
$I_S^{(f)}$, G	110	230	270	360
I_S, G	350	560	550	620
TMR, % $\vert_{H=\pm 1.4\,\mathrm{kOe}}$	1.02	2.67	4.0	0.98

obtained was a multilayer structure formed of Co island films embedded in the TiO_2 matrix (so-called discontinuous multilayer). The total thickness of $Co_x(TiO_2)_{1-x}$ composites was about 400 nm.

Static magnetic characteristics were measured by a highly sensitive vibrating sample magnetometer in the magnetic field up to 6 kOe at room temperature. Magnetization loops were measured in the film plane in two mutually perpendicular directions and normal to a film plane.

Besides, samples were explored by the ferromagnetic resonance (FMR) method in the 38–45 GHz band. The special experimental technique and the design features of experimental instrumentation are described in Ref. [6]. Both vectors of the external magnetic field and magnetic component of the extra-high-frequency field were located in the sample plane. Such arrangement of fields corresponds to the so-called "parallel geometry" of the experiment. A two-mirror open resonator was applied in the present measurements cycle as an experimental cell [6].

3. Experimental results and discussion

3.1. Static magnetic measurements

Mean saturation magnetization per unit of the film volume $I_S^{(f)}$ was determined using the in-plane magnetization loops by comparing the signal from the sample near a saturation region ($H > 5$ kOe) with the reference sample signal. After that, these data were calculated per unit of the magnetic phase volume I_S for the samples with different Co volume contents. The results are presented in Table 1. As seen from the table below, the mean saturation magnetization increases with an increase of Co concentration.

Modifications of the magnetization loops for the films with various Co contents from 31.6 to 57.6 vol% are shown in Fig. 1 for in-plane magnetization reversal (1a–d) and for perpendicular to film plane magnetization reversal (1e–h). It should be noted that the magnetization loop is the integrated characteristic of a specimen. Total magnetization at a certain field value is the weighted sum of magnetizations of each magnetic subsystem magnetized according to its intrinsic law.

Examination of in-plane magnetization loop features allows one to make the following conclusion:

1. The absence of distinctions in the magnetization loops measured in two directions in the film plane is the evidence of absence of uniaxial anisotropy in the film plane. It should be noted that at this stage of examination, we could not exclude the presence of particles (islands) that possess the shape anisotropy. These are, for example, oblong ellipsoids oriented in a random way.
2. At major magnetization cycles, we did not observe the opening of the hysteresis loops within the limits of an experimental error. Even if the magnetic phase with hysteresis is presented in the specimen, then the coercive force is less than 10–15 Oe.
3. For the samples of $X = 31.6$ vol% of Co, the dependence of reduced magnetization $I/I_S^{(f)}$ on the magnetic field H is approximated very successfully by the Langevin function:

$$\frac{I}{I_S^{(f)}} = \frac{I}{nM} = c\mathrm{th}\,X - \frac{1}{X} \equiv c\mathrm{th}\,\frac{MH}{kT} - \frac{kT}{MH}, \tag{1}$$

where I is the magnetization of sample in field H, M the particle magnetic moment, n the number of particles per volume unit, k the Boltzman constant, and T is the temperature. This fact suggests that when the in-plane magnetization reversal takes place, the 31.6 vol% Co system exhibits superparamagnetic behavior. It means that the condition of $K_{ef}V \leqslant kT$ is realized (K_{ef} is the total magnetic anisotropy constant of the particle, V is the particle volume) [7]. For our experiments at $T = 300$ K, the $K_{ef}V$ value is less than 4×10^{-14} erg.
We have calculated the magnetic moment of a superparamagnetic particle by using the congruence of the experimental and calculated magnetization curves (Fig. 2). Some definite distribution of the magnetic moments exists in the system under study. Therefore, the magnitude calculated above should be interpreted as a most probable value of the magnetic moment. The magnitude of the particle moment is $\sim 850 \times 10^{-19}$ erg/G $= 9150\,\mu_B$ (μ_B is the Bohr magneton). It is possible to evaluate the number of atoms in a magnetic particle (N) using the value of its magnetic moment M and the saturation magnetization I_S (see Table 1: $I_S = 350$ G or $0.4\,\mu_B$ per atom). This number is equal to 23 000. If we assume the particles to have a spherical shape, then their diameter should be equal to $\sim$9 nm. However, a set of spherical particles of such a diameter cannot correspond to a real situation because at vacuum deposition, the Co films become continuous with a layer whose thickness exceeds 1–2 nm [8]. Thus, the more probable particle shape is the ellipsoid (flattened spheroid) [9]. For such an ellipsoid, the ratio of vertical axes value (b) to in-plane axes value (c) should be 0.05–0.15.
4. An increase of Co content (41.4, 49.4 and 57.6 vol%) leads to the rise of the magnetization curve slope. At the same time, deviations from a canonical form of the Langevin function were observed, namely, the turn of curves to saturation became more pronounced (Fig. 1b–d). This behavior could be attributed to the appearance of particle granules having greater magnetic

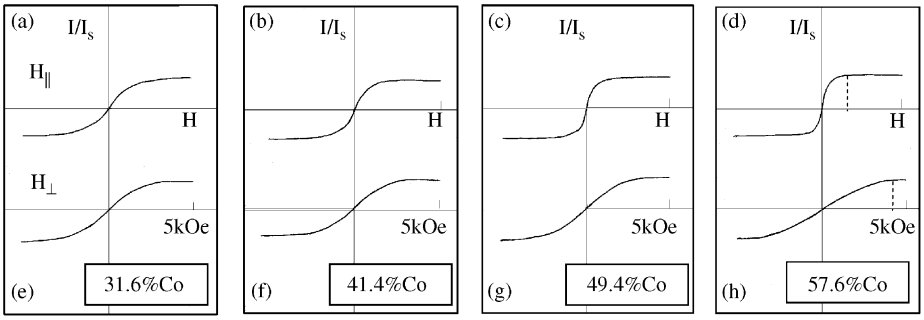

Fig. 1. Shape modification of the magnetization loops measured in the film plane (a–d) and perpendicular to the film plane (e–h) for $Co_x(TiO_2)_{1-x}$ granular composites with various Co contents. The dashed lines in Fig. 1d and h show the values of "saturation fields" H_{Spar} and H_{Sperp}, correspondingly.

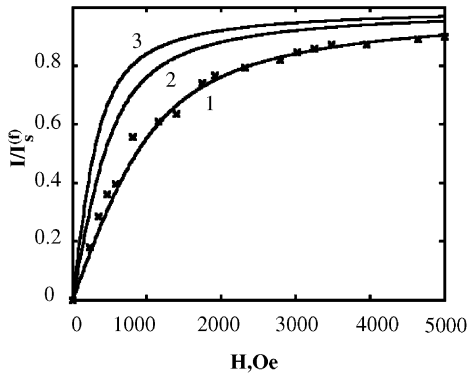

Fig. 2. Calculated magnetization curves $I/I_S^{(f)} = f(H)$ for superparamagnetic particles of various magnetic moments M: 1—$M_1 = 850 \times 10^{-19}$ erg/G; 2—$M_2 = 2M_1$; 3—$M_3 = 3M_1$ ($I/I_S^{(f)} = L(MH/kT)$ is the Langevin function). For 31.6 vol% Co films, the experimental points are denoted as crosses.

moments (see Fig. 2 where some calculated magnetization curves for superparamagnetic particles with various magnetic moments are shown). The magnetic moment of a granule increases, above all, due to the granule enlargement. It is well known [10] that during the deposition of island films, the coalescence of nearest-neighbor islands occurs. Large particles appear along with small ones. Some large granules can change their magnetic order from the superparamagnetic to the ferromagnetic single domain and then to the multidomain. So the system will consist of two subsystems: superparamagnetic and ferromagnetic. Note that in this work, we will not discuss the multidomain state of a particle since we do not detect hysteresis. As for the systems of single domain particles, the saturation state is reached at some definite field depending on the greatest K_{ef} values of granules. The contribution of this fraction leads to a more explicit turn of total magnetization curve $I/I_S^{(f)} = f(H)$ to saturation in comparison with the curves describing the ideal superparamagnetic state. It can be seen from Fig. 1b–d, "the saturation field" value H_{Spar} (i.e. the field value above that magnetization did not change noticeably) decreases gradually when Co contents rises: $\approx$2300 Oe (41.4 vol%), $\approx$2000 Oe (49.4 vol% Co) and $\approx$1600 Oe (57.6 vol% Co). There is no appropriate model to explain these values adequately. The known simple model describes non-interacting single domain particles where (1) the effective anisotropy results mainly by shape anisotropy and (2) the magnetization reversal is realized by the magnetization vector rotation. This model yields too small values of H_{Spar} (H_{Spar} = 250–700 Oe).

It is possible to get the additional information about a granule shape from the magnetization curves measured normal to a film plane (Fig. 1e–h). Note that for all samples with various Co contents, the magnetization curves differ from the Langevin function curves. The kink to saturation (not clearly explicit) can be detected on these curves of a field magnitude H_{Sperp}. As the Co concentration increases, the curve slope decreases and H_{Sperp} values grow from $\approx$3500 Oe (31.6 vol% Co) to $\approx$4500 Oe (57.6 vol% Co). For the concentration $X = 57.6$ vol% of Co, the difference in curve shapes for in-plane and perpendicular magnetization loops is similar qualitatively to the difference observed for continuous films with planar anisotropy.

These results also suggest that flattened granules (or some formations of particles with planar anisotropy) exist in the system. When the magnetization reversal process is normal to the film plane, the fraction of such granules does not exhibit the superparamagnetic behavior because the shape anisotropy (demagnetizing factor is $\approx 4\pi$) leads to the value $K_{ef}V = 2\pi I_S^2 V = 2\pi^2 I_S^2 N d^3/6$, i.e. by one order higher than kT. (In this calculation we used N = 23 000 as the number of atoms in the magnetic granule, and Co atom diameter d = 0.254 nm). Consider that such ferromagnetic granules become magnetized by the magnetization vector rotation. The total magnetization curve is the weighted sum of magnetization curves for granules characterized by various demagnetizing factors including the value of $\sim 4\pi$. Unfortunately, it is difficult to determine the kind of distribution of demagnetizing factors from the experimental data correctly. We have calculated the magnetization curve of the weighted sum of several magnetization curves for the spheroids with various demagnetizing factors. It was shown that the slope of the resulting magnetization curve decreases with the increase of the volume content of

the fraction of more flattened spheroid. On the other hand, the estimation of the largest demagnetizing factors and spheroid size parameters on the basis of H_{Sperp} and I_S values shows that the most flattened granules should exist in a sample having the smallest concentration, namely, $X = 31.6$ vol% Co ($N = 4\pi \cdot 0.8443$; axis ratio (b/c) is equal to ≈ 0.15). Further with Co content increase, the value of (b/c) should reach magnitudes of nearly ≈ 0.5.

3.2. Dynamic measurements

Granular structures were explored at $= 300$ K. The FMR lines were registered in the frequency band of 38–45 GHz. Results from these measurements are given in Fig. 3a as the resonance field–resonance frequency dependencies and as the saturation magnetization versus the concentration of Co.

The experimental dependences were approximated by the known Kittel formula in order to find the magnetization saturation. This formula for the given geometry of experiment [11] is:

$$v_{\text{res}} = \frac{g\mu_B}{h}\sqrt{H_{\text{res}}(H_{\text{res}} + 4\pi I_S)}, \tag{2}$$

where v_{res} is the resonant frequency, g the spectroscopic splitting factor (usually it is considered that $g = 2.05 \pm 5\%$, see for instance Ref. [12]), μ_B is the Bohr magneton, h is the Plank constant, H_{res} is the resonant magnetic field, and I_S is the saturation magnetization.

The magnitudes of I_S obtained from Eq. (2) are presented as a function of the concentration of Co granules in the sample (Fig. 3b). One can see from this figure that higher the concentration of metal phase, stronger the magnetization. The extrapolation of these data demonstrates that for the concentration of Co granules $X = 100\%$, the magnetization should achieve the value of 800 G. Let us note that this magnitude is less essential than for bulk Co ($\text{Co}_{100} = 1420$ G). Moreover, this fact is not surprising as the investigated objects are quasi-two-dimensional. An exchange interaction between spins of a ferromagnetic appears smaller than in the three-dimensional case for such objects. It should be also noted that the dependence of the saturation magnetization on the concentration of magnetic granules obtained by dynamic and static methods is qualitatively similar. However, some distinctions in numerical data, which exceed an error of the experiment, are observed. Probably it is caused by the fact that the influence of shapes and sizes of Co magnetic granules was not taken into account in the calculations. In the following section, the qualitative analysis of the dependence of magnetic properties of a granular structure on the size and shape of magnetic granules is given.

3.3. Determination of granules shape

The purpose of the given section is to define the shape of granules in the magnetic structure $\text{Co}_x(\text{TiO}_2)_{1-x}$, from the results of the FMR data.

In particular, the results of the calculations for one of the explored specimens $\text{Co}_x(\text{TiO}_2)_{1-x}$ with the concentration of the magnetic granules $X = 31.6\%$ are given below. In the beginning, we assume that the magnetic particles embedded in the sample appear as thin plates. Their planes coincide with the plane of the sample. Thus, demagnetizing factors [13] for the sample are equal to $N^{(x)} = N^{(z)} = 0$, $N^{(y)} = 4\pi$. In our experiment, the permanent and alternative fields lie in the plane of the sample and are mutually orthogonal. Such arrangement of the experiment justifies an application of formula for searching the resonant frequency magnitude v_{res}. Then, substituting the experimentally obtained values H_{res} and v_{res} in (2), we have calculated the saturation magnetization of the given sample $I_S = 447$ G.

Now let us try to define the possible shapes of the particles in the sample to which the same set of quantities (H_{res}, v_{res} and I_S) can be assigned. As shown above, the technology of the preparation allows us to describe the sample as a system consisting of ellipsoidal magnetic granules.

In order to do it, let us write the Kittel formula for a general case [11]:

$$v_{\text{res}} = \gamma\{[(N^{(x)} - N^{(z)})I_S + H_{\text{res}}][H_{\text{res}} + (N^{(y)} - N^{(z)})I_S]\}^{1/2}, \tag{3}$$

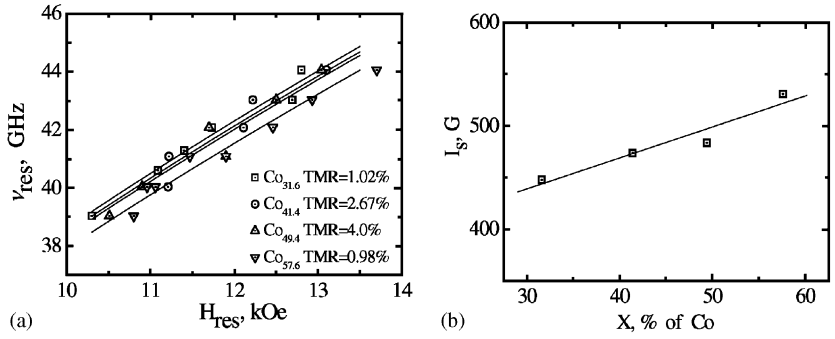

Fig. 3. Data of the FMR investigations in 38–45 GHz band at $T = 300$ K. (a) The resonance frequency–resonance field dependence for $\text{Co}_x(\text{TiO}_2)_{1-x}$, (b) the saturation magnetization versus the concentration of Co granules in the specimen.

where I_S is the saturation magnetization of substance, γ the gyromagnetic ratio, H_{res} the resonant field and $N^{(x)}$, $N^{(y)}$, $N^{(z)}$ are demagnetizing factors along OX, OY, OZ axes, correspondingly. Let us solve this equation for H_{res}, using the experimental values ν_{res} and substituting I_S, calculated into (2). We assume demagnetizing factors $N^{(x)}$, $N^{(z)}$, $N^{(y)}$ as parameters taking into account the shape of the explored particle. For this purpose, let use the formula (4) obtained in Ref. [12]:

$$N^{(x)} = \frac{abc}{2}\int_0^\infty \frac{ds}{(s+a^2)\sqrt{(s+a^2)(s+b^2)(s+c^2)}},$$
$$N^{(y)} = \frac{abc}{2}\int_0^\infty \frac{ds}{(s+b^2)\sqrt{(s+a^2)(s+b^2)(s+c^2)}},$$
$$N^{(z)} = \frac{abc}{2}\int_0^\infty \frac{ds}{(s+c^2)\sqrt{(s+a^2)(s+b^2)(s+c^2)}}, \quad (4)$$

where a, b, c are the semi-axes of the ellipsoid in OX, OY, OZ directions, correspondingly. Varying a, b, c, we change the shape of the ellipsoidal particle from strongly extruded in the sample plane to strongly flattened along the normal to the sample plane. The obtained results are given as the diagram of the dependence of magnitude H_{res} on the relation between the semi-axes of the ellipsoid (Fig. 4, curve 1) for the frequency $\nu_{res} = 40$ GHz. It is easy to see that the point on the abscissa axis where $b/c = 1/1$ corresponds to the situation $a = b = c$ (i.e. to the spherical shape). While moving left from the point ($b/c = 1/1$), we shift to the area of the particles that are more and more compressed along OY-axis. In the limit of $b/c \to 0$ (at $c = a$, $b = \text{const}$), we have the thin-film shape of the specimen. While moving right from the point ($b/c = 1/1$), we shift to the area of the particles that are more and more elongated along OZ–axis. In the limit of $b/c \to 0$ (at $b = a = \text{const}$), we have a wire-like shape of the particles.

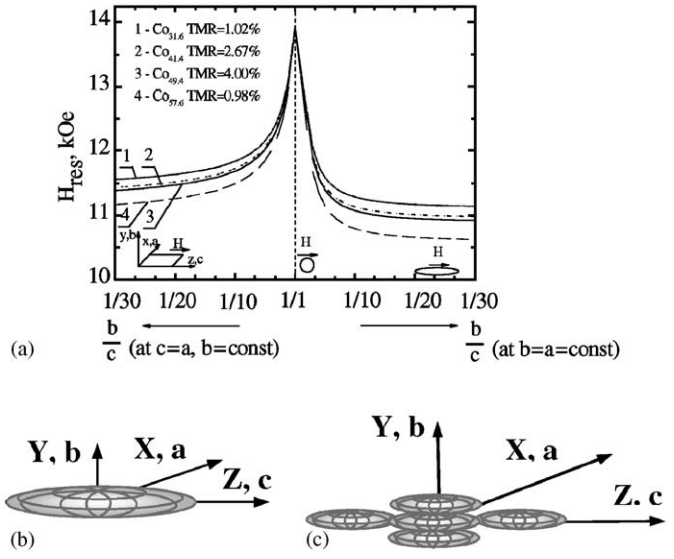

Fig. 4. Manifestation of particles' shape in the FMR response for $Co_x(TiO_2)_{1-x}$ nanocomposites with various X%. (a) Dependencies of resonant fields on the ratio between ellipsoidal particles' semi-axes, (b) shape of the separate granuleand (c) the proposed shapes of the effective cluster.

As seen from Fig. 4, two points on the abscissa axis (curve 1) correspond to only one magnitude of the resonance field H_{res}. This situation can be interpreted as follows: there are magnetic granules which have the shape, both plate and the ellipsoidal ones with $b/c = 1/6-1/7$. Note that similar results are obtained for the other Co concentrations, and for all of them, two points on the abscissa axis correspond to only one magnitude of the resonance field H_{res}.

The results obtained by a static method allow one to suggest that Co particles in the samples under study have the shape of spheroids flattened in a normal direction to the film plane (along OY-axis, i.e. $b<a$; at $a = c$, see Fig. 4(b) and (c)). The ratio of axes for the separate spheroid has been estimated as $b/a<0.15 \approx 1/6$, i.e. ($a \times b \times c = 6 \times 1 \times 6$). It has turned out that it is difficult to explain the numerical values of "fields of saturation" (H_{Sper} and H_{Spar}) using the conception of non-interacting particles. It is possible to assume that some interaction between adjacent particles takes place. This interaction leads to an antiparallel arrangement of magnetization vectors. Thus, the magnetic field of the larger amplitude will be required for the in-plane magnetic saturation. On the other hand, when magnetizing in the direction normal to the film plane, such "chains" require smaller fields for saturation due to the magnetostatic coupling. In other words, "chains" have the smaller effective demagnetizing factor than separate particles.

As a hypothesis describing the magnetic structure of the explored granular nanocomposites, we can present the following consideration:

The magnetic interaction between particles leads to the formation of clusters with the short-range magnetic order. It should be noted that an opportunity of the formation of the similar magnetic structure ("superferromagnetism" caused by the interaction of superparamagnetic particles) was also discussed in Refs. [5,14]. Let us assume that the coordination number equal to 4 characterizes such a short-range magnetic order. Then, the magnetic chains consisting of three interacting particles will be formed in the direction normal to the film plane (Fig. 4c). In the film plane, in the direction of the applied magnetic field, the "chains" consisting of three particles will be formed as well. If the effective size of a single particle expressed in arbitrary units is equal to $6 \times 1 \times 6$ (Fig. 4b), then the size of the appeared cluster will be equal to $6 \times 3 \times 18$, that corresponds to the ratio between axes $2 \times 1 \times 6$ (Fig. 4c). As a first approximation, the given cluster can be approximated by an ellipsoid with the ratio of axes $a/b/c = 2/1/6$. The electron spin resonance field calculated for such an ellipsoidal cluster differs by 2% from the field of the electron spin resonance calculated for the ellipsoidal particle with a ratio

of axes 1/1/6 that was obtained from the analysis of the FMR data (Fig. 4a).

4. Conclusions

Static and dynamic (FMR) examinations of the magnetic properties of nanocomposites with various concentrations of magnetic phase were carried out to obtain the detailed information regarding the interior structure and magnetic interactions in Co–Ti–O granular nanocomposites. The comparison of the results obtained by these methods was performed as well.

1. Both applied methods show that in spite of some quantitative distinctions, the saturation magnetization of explored magnetic nanostructures is less than the magnetization for a bulk material. It increases with a rise of volumetric content of Co.
2. It is shown that the samples with 31.6 vol% Co exhibit superparamagnetic behavior under the in-plane magnetization reversal. As the Co contents increase, the ferromagnetic phase appears along with the superparamagnetic phase. The samples do not exhibit superparamagnetic properties at the magnetization reversal perpendicular to the film plane.
3. The estimation of the most probable size and shape parameters of particles was performed. It is shown that the number of atoms in a single particle exceeds 23 000. The particles can be presented as oblate spheroids with a ratio of the small axis to the large one of less than $\sim$0.15.
4. The model of the granular system that contains clusters consisting of several interacting particles with the short-range magnetic order is suggested.

Acknowledgment

The authors are grateful to Prof. A.B. Granovsky (Moscow State University) for the provision of samples. The work is partially supported by the grant STCU #1916.

References

[1] H. Fujimori, S. Hitani, S. Ohnuma, Mater. Sci. Eng. B 31 (1995) 219.
[2] E. Gan'shina, A. Granovsky, B. Dieny, M. Kumaritova, A. Yurasov, Physica B 299 (2001) 260.
[3] N. Kobayashi, S. Ohnuma, T. Masumoto, H. Fujimori, J. Appl. Phys. 90 (2001) 4159.
[4] A. Granovsky, A. Kozlov, T. Bagmut, S. Nedukh, S. Tarapov, J. Clerc, Phys. Solid State 47 (4) (2005) 738.
[5] M. Knobel, W. Nunes, A. Brandl, J. Vargas, L. Socolovsky, D. Zanchet, Physica B 354 (2004) 80.
[6] S. Tarapov, T. Bagmut, A. Granovsky, V. Derkach, S. Nedukh, A. Plevako, S. Roschenko, I. Shipkova, Int. J. Infrared Millimeter Waves 25 (11) (2004) 1581.
[7] M. Li, G.-C. Wang, J. Magn. Magn. Mater. 217 (2000) 199.
[8] S. Vonsovskij, The Magnetism M, 1971, 1032pp (in Russian).
[9] R. Bozorth, Ferromagnetism, D. Van Nostrand Co., Princenton, 1951.
[10] L.I. Maissel, R. Glang (Eds.), Handbook of Thin Film Technology, McGraw Hill Hook Company, 1970.
[11] E. Borovik, A. Mil'ner, V. Eremenko, Lectures on Magnetism, Edit House Kharkov University, 1972, p. 248 (in Russian).
[12] D. Belozorov, V. Derkach, S. Nedukh, A. Ravlik, S. Roschenko, I. Shipkova, S. Tarapov, F. Yildiz, B. Aktas, J. Magn. Magn. Mater. 263 (2003) 315.
[13] D. Landau, E. Lifshitz, Electrodynamics of Continuous Media, vol. 8, Edit House M Science, 1982, p. 621 (in Russian).
[14] J. Benardin, A. Brandl, M. Knobel, P. Panisodd, A. Pakhomov, Y. Liu, X.X. Zhang, Phys. Rev. B 65 (2002) 64422.